Summer 8-5-2019

Design and Analysis of Modular Axial Flux Switched Reluctance Motor

Rochak Shiwakoti
University of New Orleans, rshiwako@uno.edu

Design and Analysis of Modular Axial Flux Switched Reluctance Motor

A Thesis

Submitted to the Graduate Faculty of the
University of New Orleans
in partial fulfillment of the
requirements for the degree of

Master of Science
in
Engineering
Electrical Engineering

by

Rochak Shiwakoti

B.S. University of New Orleans, 2016

August, 2019

Acknowledgment

The work presented in this thesis could not be a reality if not for the guidance, support, patience of many people. I would like to extend my gratitude first to my thesis advisor Dr. Ebrahim Amiri for his continuous guidance and instructions throughout my graduate career.

I would additionally like to thank Dr. Rastgoufard and Dr. Ittiphong Leevongwat for providing their insight and evaluation to my work periodically. I would also take this opportunity to thank them for being the member of my thesis committee.

I would like to thank my friend and co-worker Bikrant Poudel for sharing his experiences that helped me with my work.

I would like to dedicate this work to my family and my girlfriend for their continuous trust and support to make the completion of my work possible.

Contents

List of Figures v

List of Tables vii

Abstract viii

1 Introduction 1

1.1 Radial flux Switched Reluctance Motors 1

1.2 Axial Flux Switched Reluctance Motor 1

1.3 Research Objective 3

2 Literature Review 4

2.1 Design Structure and Characteristics of Axial Flux Switched Reluctance Motor 4

2.2 Inductance of Axial Flux Switched Reluctance Motor 5

2.3 Torque of Axial Flux Switched Reluctance Motor 6

2.4 Ohmic loss 7

3 Proposed Motor 9

3.1 Structure of the Proposed Axial Flux Switched Reluctance Motor 9

3.2 Excitation Current & Design Parameters 9

3.3 Wire Dimension 10

3.4 Structure of Stator winding 10

3.5 Phase Excitation Sequence 11

4 ANSYS Maxwell 12

4.1 ANSYS Maxwell 3D 13

4.2 ANYSYS Simplorer 14

5 Magentostatic Simulation 16
5.1 Proposed AFSRM-Single layer Simulation 17
5.1.1 Single layer single phase excitation 17
5.1.2 Single layer all phase sequentially excitation 19
5.1.3 Double layer single phase excitation 21
5.1.4 Double layer all phase sequentially excitation 22
5.1.5 Four layer single phase excitation 23
5.1.6 Four layer all phase sequentially excitation 25
5.2 Torque Comparison 27
5.3 Conventional AFSRM Simulation 28
5.4 Comparison between proposed four stack AFSRM and conventional stack motor 29

6 Transient Simulation 31
6.1 Design of Drive System 31
6.2 Drive System Using Ansys Simplorer 32
6.3 Current Profile 32
6.4 Torque Profile 34
6.5 Radial Force 35

7 Conclusion & Future Works 37

Bibliography 40

Appendix 41

Vita 52

List of Figures

1.1 A 6/4 Switched Reluctance Motor [1] 2

1.2 An Axial Flux Switched Reluctance Motor 2

3.1 Exploded view of proposed motor 9

3.2 Stator winding structure of the Axial Flux SRM. 11

3.3 Stator winding excitation sequence. 11

5.1 Torque developed at different rotor position with Phase A excited for one layer 17

5.2 Inductance at different rotor position with Phase A excited for one layer 18

5.3 Radial Force experienced by the whole motor at different rotor position with Phase A excited for one layer 18

5.4 Torque at different rotor position with 3 Phase excitation for one layer 19

5.5 Inductance at different rotor position with 3 Phase excitation for one layer 19

5.6 Radial force at different rotor position with 3 Phase excitation for one layer 20

5.7 Torque developed at different rotor position with Phase A excited for double layer . 21

5.8 Inductance at different rotor position with Phase A excited for double layer 21

5.9 Radial Force experienced by the whole motor at different rotor position with Phase A excited for double layer 22

5.10 Torque at different rotor position with 3 Phase excitation for double layer 22

5.11 Inductance at different rotor position with 3 Phase excitation for double layer 23

5.12 Radial force at different rotor position with 3 Phase excitation for double layer 23

5.13 Torque developed at different rotor position with Phase A excited for four layer 24

5.14 Inductance at different rotor position with Phase A excited for four layer 24

5.15 Radial Force experienced by the whole motor at different rotor position with Phase A excited for four layer 25

5.16 Torque at different rotor position with 3 Phase excitation for four layer 25
5.17 Inductance at different rotor position with 3 Phase excitation for four layer 26
5.18 Radial force at different rotor position with 3 Phase excitation for four layer.....26
5.19 Characteristic of motor torque of proposed modular motor with 4 layers excitation . 27
5.20 Torque at different rotor position with 3 Phase excitation for conventional AFSRM . 28
5.21 Inductance at different rotor position with 3 Phase excitation for conventional AFSRM 28
5.22 Radial force at different rotor position with 3 Phase excitation for conventional AFSRM 29

6.1 Axial Flux Switched Reluctance motor drive system. 31
6.2 Data flow between FEA software and the circuit design tool. 32
6.3 The profile of the phase current in the proposed motor. 33
6.4 The profile of the phase current in the conventional motor. 34
6.5 Transient torque profile of the proposed motor Vs the conventional motor. 34
6.6 Radial force of the proposed motor Vs the conventional motor. 35

List of Tables

3.1 Motor Data.....10

3.2 Diameter and Resistance of 12 AWG copper cable 10

5.1 Magnetostatic results comparison for proposed motor and conventional motor 29

6.1 Transient torque results comparison for proposed motor and conventional motor.....35

6.2 Transient radial force results comparison for proposed motor and conventional motor 36

Abstract

This thesis presents a new modular structure of the axial flux Switched Reluctance Motor (SRM). The design consists of four stator disks with each adjacent disk rotated 30 degrees apart and four rotor disks connected to a common shaft. The proposed design aims to reduce the unwanted radial force, mitigate the torque ripple, and improve the efficiency. The modular structure distributes the radial force and torque strokes along the axial length of the motor, potentially damping the torque pulsation. In addition, the modular structure would deliver the rating power at a lower current level, reducing the ohmic loss. When fault occurs on a motor disk or its control unit, the motor would still operate through other disks, increasing the reliability of the system. The effectiveness of the proposed design, the magneto-static and transient performance of the motor are compared with the conventional single layer structure using 3-D Finite-Element software tool.

Keywords: Axial flux, Modular structure, Torque Ripple, Radial force, Switched Reluctance Motor, Finite Element Analysis, Cosimulation

Chapter 1

Introduction

1.1 Radial flux Switched Reluctance Motors

Switched Reluctance Motors (SRM) have advantages such as a very simple structure with no winding in the rotor side [2]. It has a high tolerances, robustness and it is low cost with no permanent magnet in the structure [2, 3]. It can operate in high temperature and in intense temperature variations [4]. Switched reluctance motor operates due to reluctance torque [4]. In other words, torque is produced in SRM because of the tendency of the rotor poles to align with excited stator poles [3]. This is based on the difference in reluctance path for the magnetic field lines between the aligned and unaligned rotor position [2]. When a stator pole is excited, an unaligned rotor experiences a force and gets attracted to the excited stator pole thereby creating torque [3]. However, because SRM has salient poles and has non linear magnetic characteristics, it faces the problems of noise and torque ripple more than other contemporary motors [2]. The torque ripple is inherent drawback of SRMs [4] and it is caused by geometric structure of the motor itself [4].

The rotor of SRM is mostly laminated steel shaped to form salient poles [3]. The number of stator poles in SRM is higher than number of rotor poles so that at every position of the rotor, initial torque can be produced [2]. Following figure shows a 6/4 SRM

1.2 Axial Flux Switched Reluctance Motor

The electric motors that operates on the reluctance property are further categorized into different types by the nature of the magnetic field path as to its direction with respect to the axial length of the machine [5]. When the path of magnetic field is perpendicular to the rotor shaft, the motor is classified as radial field switched reluctance motor [5]. The motor whose flux path is along the axial direction, are called axial flux switched reluctance motors (AFSRM). Following figure shows

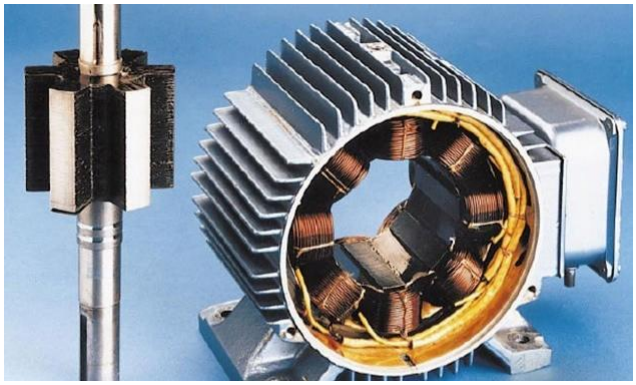

Figure 1.1: A 6/4 Switched Reluctance Motor [1]

a 6/4 SRM configuration.

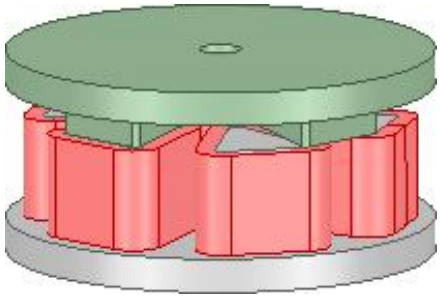

Figure 1.2: An Axial Flux Switched Reluctance Motor

The flux path of this motor is through the upper stator pole tip, air gap, upper rotor pole tip back to the airgap and again to the stator pole tip. When multiple of such single stack AFSRMs are arranged on a single shaft to increase the power ratings, they are known as multiple-stack axial flux switched reluctance motor [5].

In the recent couple of years, large number of research have been done to find the potential and feasible industrial and commercial applications of Electric Vehicles [6, 7, 8]. Permanent magnet motors are popular but they are very rare and have international market problem [6, 9]. The control of Induction Machines is difficult and they also have a complex structure [6]. Most focus have been given to SRM due to its simple, rugged and reliable structure [3, 6]. These motor solely operates based on reluctance torque with zero amount of PMs [10]. Axial flux type motors are more feasible in traction application where high radial space and limited axial space is available [11, 12].In particular, in-wheel drive in electric vehicle is a very feasible application of AFSRMs [7].

Unlike Single Phase induction Motors (SPIMs) are widely used for residential applications such as heat pump loads [13], SRMs are not widely used commercially. This thesis is aimed at researching and studying the disadvantages of axial flux switched reluctance motor with an aim of mitigating them so that it can be more useful for application in in-wheel drive of Electric Vehicles. In this thesis, a multiple-stack axial flux SRM is compared with a conventional single stack AFSRM to see if the former is more feasible and applicable for industrial and commercial use.

1.3 Research Objective

The main objective of this research is to design a modular AFSRM to have lesser torque ripple, radial forces and ohmic losses than conventional single stack AFSRM. The other objectives of the research are as follows:

1. To study conventional axial flux switched reluctance motors (AFSRM).
2. To propose a design for a modular stack AFSRM that has better performance than a conventional single stack AFSRM.
3. To model proposed modular and conventional AFSRM in a 3D FEA software tool.
4. To perform magneto-static analysis on both conventional and proposed AFSRM to achieve:
    - Torque
    - Radial Force
    - Inductance
5. To verify magneto-static torque and inductance profile analytically.
6. To perform transient analysis on both conventional and proposed AFSRM.
7. To compare conventional and proposed AFSRM with each other to see which one has better performance in terms of
    - torque ripple
    - radial force
    - ohmic loss

Chapter 2

Literature Review

2.1 Design Structure and Characteristics of Axial Flux Switched Reluctance Motor

Switched reluctance motors (SRMs) are getting special attention due to their simple structure, high reliability and a large torque over a wide range of speed [14]. However, SRMs have their own shortcoming, which includes acoustic noise generation and high torque ripple [15]. Due to its advantage of simple and rugged structure, low cost, high reliability robust performance and fault tolerance SRMs are expected to be applied to Electric Vehicle applications [7].Nowadays, axial flux electric motors are considered for some applications especially where a large diameter/axial length ratio is required.

Axial flux Switched Reluctance Motors (SRMs) are among the most reliable, robust, fault tolerant, and high power density electric machines with a wide range of operating speed. Such motors are potentially an appropriate choice for applications where a large diameter/axial length ratio is required [11, 12], such as in-wheel propulsion electric vehicle (EVs) [14, 7] However, due to their salient structure[16] and non-linear magnetic characteristic, such motors suffer fromlarge torque/force ripple [15].

There are primarily two methods for keeping the torque ripple whiten the permissible limits; one method is to modify and optimize the geometric structure and the magnetic design of the motor [17, 18], while the other is to use advanced motor drive techniques [19]. However, the methods available in the literature are mainly developed for radial flux SRMs.

This thesis, presents a new design for axial flux SRM to lower the torque ripple and improve the overall efficiency. The proposed design is based on a modular structure with four stator/rotor disks. To effectively distribute the rotational torque along the axial length of the motor, every two non-adjacent stator disks (stator 1 & 3, stator 2 & 4) are excited synchronously. The motor

performance is analyzed via Finite Element (FE) and compared with the conventional single disk axial flux SRM.

2.2 Inductance of Axial Flux Switched Reluctance Motor

Torque generated in Switched Reluctance Machine is the function of inductance [5, 14]. Thus, SRM operation can be best explained with the help of inductance [5, 14].

In Magnetic circuits, Magneto motive force (F) is given by [5, 14]

$$F = \varphi * R \tag{2.1}$$

Where φ is Equivalent Flux and R is Magnetic Reluctance. And φ is given by [5, 14]

$$\varphi = \frac{\lambda}{N} \tag{2.2}$$

Where λ (=L*i) is flux linkage, N is number of turns, L is inductance and i is current.

From equations (3.1) and (3.2) we can write [5, 14],

$$F = \frac{\lambda}{N} * R \tag{2.3}$$

$$Ni = \frac{\lambda}{N} * R \tag{2.4}$$

$$N^2 = \frac{\lambda}{i} * R \tag{2.5}$$

$$N^2 = LR \tag{2.6}$$

$$L = \frac{N^2}{R} \tag{2.7}$$

Thus, it can be said Phase Inductance of the coil is inversely proportional to magnetic reluctance [5, 14].

When the rotor poles in the two halves of the rotor are aligned , the phase inductance of the 6/4 AFSRM can be modeled using the Fourier series as follows.

$$L(i, \theta) = L_0(i) + L_1(i) * cos(P_r * \theta) + L_2(i) * cos(cos(2 * P_r * \theta)) \quad (2.8)$$

$$L_0(i) = \frac{1}{2}[\frac{1}{2}(L_a + L_u) + L_m] \quad (2.9)$$

$$L_0(i) = \frac{1}{2}(L_a - L_m) \quad (2.10)$$

$$L_2(i) = \frac{1}{2}[\frac{1}{2}(L_a + L_u)] \quad (2.11)$$

where, θ is the rotor position, i is the phase current, Pr is the number of rotor poles, La and Lu are the inductance values at the aligned and unaligned positions respectively and Lm is the inductance at the midway between the unaligned and aligned positions.

The value of L_a is given by:

$$L_a = \frac{N^2}{(R_g + R_m)} \quad (2.12)$$

The value of L_u is given by:

$$L_u = \frac{N^2}{R_g} \quad (2.13)$$

where N= number of turns, Rg= Resistance of the airgap and Rm= resistance of the motor body through which the flux passes.

2.3 Torque of Axial Flux Switched Reluctance Motor

Torque is often represented in terms of current rather than flux and also in terms of co-energy rather than energy [5]. The calculation of electromagnetic Torque is often in terms of magnetic nonlinear system terms of co-energy W^j as [5, 14].

$$T(\theta, i) = \frac{\partial W^j(\theta, i)}{\partial \theta} \quad (2.14)$$

where θ is angular position of rotor and i is current flowing through the coil. Co-energy depends on θ and instantaneous value of current [5].

At any θ , W^j is the region under the magnetization curve and it can be stated as [5, 14, 20].

$$W' = \int_0^{i} \varphi(\theta, i)\, di \tag{2.15}$$

Now Combining From 3.14 and 3.15

$$W' = \int_0^{i} L(\theta).i\, di \tag{2.16}$$

$$W' = \frac{i^2}{2} * L(\theta) \tag{2.17}$$

Hence, the reluctance torque of SRM is resulted from the tendency of moving the rotor poles in line with energized stator pole to maximize the inductance of the excited coil can be expressed as [5, 14, 20] :

$$T = \frac{i^2}{2} * \frac{dL}{d\theta} \tag{2.18}$$

For the proposed modular full stack the overall torque is obtained by [19]:

$$T_{total} = \frac{1}{2} \sum_{k=1}^{P_s} i^2{}_k * \frac{dL_k}{d\theta} \tag{2.19}$$

where, T_{total} is overall torque, P_s is number of stator phases excited, i_k = is the excitation current, θ is the mechanical angle of the rotor, $L_k(\theta)$ is the inductance of the k^{th} disk obtained from equation 3.8.

2.4 Ohmic loss

In regards to the motor efficiency, the proposed structure can significantly decrease the stator winding ohmic loss. Based on Eqs(2.20, 2.21), the ohmic loss is proportional to the square of the current. Although, the overall wiring length in the proposed 4-layer structure is quadruple of that in the conventional 1-layer structure, the stator current is four times less. Therefore, the ohmic loss in the proposed structure would be less according to Eqs(2.20, 2.21) The Ohmic loss of the conventional structure P_{cop} and proposed motor $P_{cop.new}$ are:

$$P_{cop} = R * I^2 \tag{2.20}$$

$$P_{cop.new} = 4 * R * (\frac{I}{4})^2 \tag{2.21}$$

In rated current 76.9A, ohmic losses ratio is obtained as:

$$\frac{P_{cop}}{P_{cop.new}} = 4 \tag{2.22}$$

Chapter 3

Proposed Motor

3.1 Structure of the Proposed Axial Flux Switched Reluctance Motor

Axial flux SRMs are doubly salient, singly excited types of motor with the winding being located only on the stator side, similar to radial flux SRMs. Based on the position of the rotor poles, stator poles are sequentially excited to provide a continuous positive torque. The proposed modular structure consists of four stator disks shifted by 30 degrees and four rotor disks connected to a common shaft as shown schematically in figure below. The stator disks are shifted in order to arrange an interleaved torque/force profile among the group of four disks and, thereby, effectively reducing torque ripple and vibration [21].

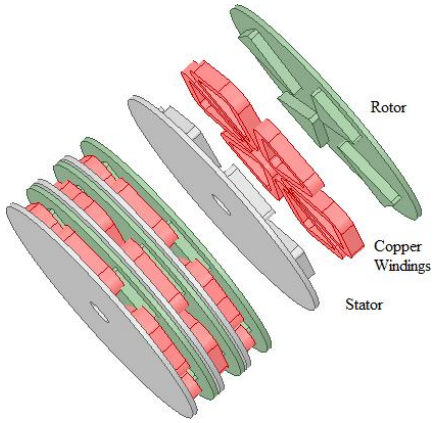

Figure 3.1: Exploded view of proposed motor

3.2 Excitation Current & Design Parameters

The motor is primarily designed for in-wheel propulsion EV application. For this purpose, the motor is supplied by 650V battery to deliver the rated power of 50 kW. Since the structure is composed of four disks, each disk is designed to deliver 12.5 kW. The rated current of the stator

winding is given by:

$$I = \frac{P}{V} \tag{3.1}$$

where, P is the rating power per disk and V is the battery voltage. As observed in Fig. 2, phase windings are separated by 10 to 11 mm air gap to avoid accidental electrical contact between the two windings. The basic design data of the motor for both conventional and proposed motor is enclosed in table below.

Table 3.1: Motor Data

	Parameter	4 Stack (mm)	Single Stack(mm)
Stator	Outer diameter	508	508
	Stack length	40/stack	160
	Number of poles	6	6
Rotor	Outer diameter	508	508
	Inner diameter	50	50
	Number of poles	4	4
	Stack Length	20 /stack	80 mm
	Air gap	0.25	0.25
Excitation	Current	19.23A/stack	76.92A

3.3 Wire Dimension

For the required current rating, 12 AWG wire was used. The ampacity of 12 AWG is 25 A which is 5 A above the required current rating as a safety factor. The following table shows the diameter and resistance of the 12 AWG copper winding cable.

Table 3.2: Diameter and Resistance of 12 AWG copper cable

AWG	Conductor Diameter(mm)	Ohms/mm.	Ohms/Km(%)
12	2.05232	0.00000520864	5.208640

3.4 Structure of Stator winding

The stator tooth height is 30 mm and the winding width around the stator is 23 mm. It is made sure that the winding width is 23mm so that there is about 10 to 11mm air gap between the two stator winding to avoid accidental electrical contact between the two windings. The winding width can accommodate about 115 turns of 12 AWG in 16.5mm and extra 6.5 mm (16.5mm+6.5mm=23mm) width is left for winding insulation. So, there will be 115 turns in the stator winding.

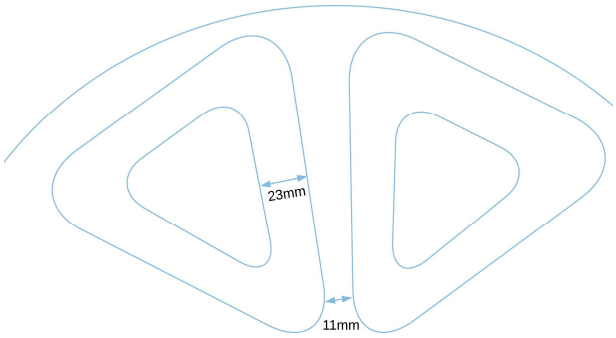

Figure 3.2: Stator winding structure of the Axial Flux SRM.

3.5 Phase Excitation Sequence

To effectively reduce the undesirable radial forces stator 1 is excited synchronously with stator 3, while stator 2 operates in synch with stator 4. Figure below shows the proposed switching sequence for stators 1 and 2.

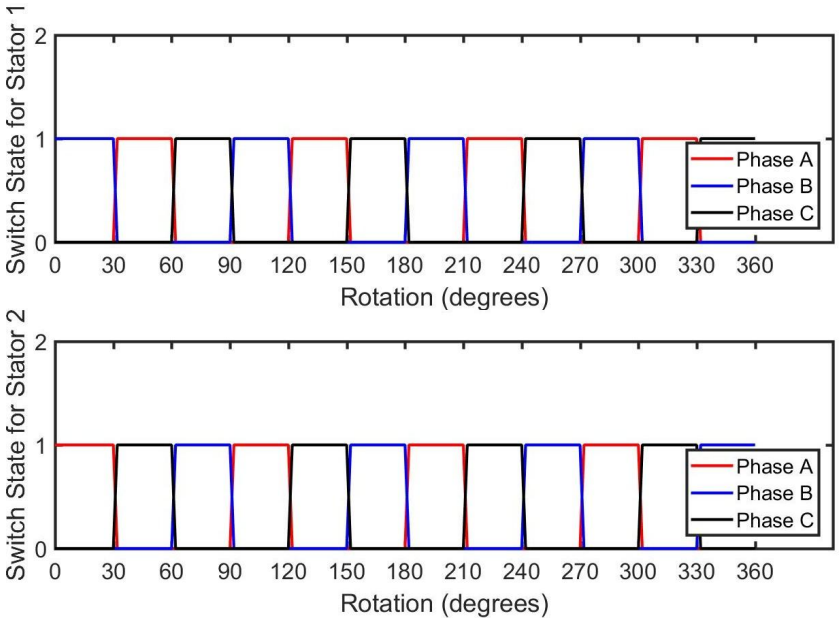

Figure 3.3: Stator winding excitation sequence.

Chapter 4

ANSYS Maxwell

ANSYS is a design and simulation software that is developed by Ansys Inc [22, 23].It is mostly used in product design phase to carry out Finite Element Analysis (FEA) test, vibrational analysis test and also electromagnetic analysis test [22, 23]. ANSYS Maxwell is a product of ANSYS that uses FEA to solve electrostatic, magnetostatics, eddy current and transient problems [22, 23]. This software is used to solve electromagnetic field problems in motors, transformers and other electric machines by solving Maxwell ' s equation. The Maxwell equation is solved in the finite region of space specified by the user with the suitable boundary conditions [22, 23].

Initially the geometry is defined based on the problem and the defined geometry is divided into many basic/fundamental elements [22, 23]. These elements are known as finite element mesh of the geometry. The differential equations related to the electromagnetic process are solved in each of this geometrical elements using the Maxwell equations.

James Clerk Maxwell, a Scottish scientist combined Ampere ' s Law, Faraday ' s Law, Gauss Law to create four equations to form fundamental of classic electromagnetism [23]. The principles of electromagnetic system can be predicted by using the mathematical equitation combined by Maxwell.

Using mathematical formulation given by him, principles governing electromagnetic system can be defined [22]. These mathematical equations define electric and magnetic forces involved in electromechanical conversion process [23]. These four Maxwell equations [23, 24] that define electromagnetic field are briefly discussed below:

The equation below is also known as the Gauss ' s law [23, 24]. Gauss law stats that the divergence of the electric flux density over any region is always equal to the amount of charge in the region [23, 24].According to this law electric charge acts as sources or sinks for electric fields [23, 24].

Gauss Law for Magnetism [23, 24]

$$Q.D = \rho \tag{4.1}$$

Where Q= Divergence operator, D = Electric flux density and ρ = Charge density

Equation below is the second Maxwell ' s Equation and is known Gauss Law for Magnetism [23, 24].According to this law, magnetic monopoles does not exist in the universe [23, 24]. The equation interprets divergence of magnetic field is zero through any region [23, 24].

$$Q.B = 0 \tag{4.2}$$

where B = Magnetic field

Equation below is the third Maxwell ' s equation and is known as Faraday ' s Law [23, 24]. According to this law, change in magnetic flux within a closed loop of wire produces voltage across the wire [23, 24]. Faraday ' s Law of induction [23, 24]

$$QXE = \frac{-\partial B}{\partial t} \tag{4.3}$$

where E = Electric field

Equation (30) is the fourth Maxwell ' s equation and is known as Ampere ' s law [23, 24]. According to this law, electric current flowing through the wire produces magnetic field that circles the wire [23, 24].

Ampere ' s Law [23, 24]

$$QXH = \frac{\partial D}{\partial t} + J \tag{4.4}$$

4.1 ANSYS Maxwell 3D

Maxwell is a high-performance interactive software package that uses finite element analysis (FEA) to solve three-dimensional (3D) electric, magnetostatic,eddy current, and transient problems [25]. To solve the sect of algebraic equations the geometry of the problem is divided into small three dimensional tetrahedron [26]. The combination or the group of the tetrahedrons is referred as mesh [26]. In Maxwell 3D, there are solution types that needs to be chosen before starting a project

[25, 26]. The following are the Maxwell solution types that can be solved using the Maxwell 3D package [25, 26].

The characteristics of the solution set up types are classified and discussed briefly below [26]:

- Magnetostatic: It deals with the static magnetic forces, inductance, magnetic fields and torque that are causes by non- alternating currents, static external magnetic fields or PMs. It can be used for both linear aor non linear materials.
- Eddy current: It deals with the sinusoidal varying magnetic fields,forces impedance and torque .The induced fields like skin effects and proximity effects are considered and it is used for linear materials only.
- Transient Magnetic: This solution types solves transient magnetic field caused by time varying or moving electrical sources and PMs. The sources can be DC, transient voltage or currents. In this set up, we can link external circuit with the 3D model or create a link to Simplorer.
- Electrostatic: This solution types is used for static electric fields, forces, torques that are caused by charges or voltage distribution over linear materials.
- DC Conduction: It solves the DC current distribution in conducting materials.
- Transient Electric: This set up computes time varying electric field that are causes by the time varying voltages, charge distributions or current excitation in non linear materials.

4.2 ANYSYS Simplorer

ANSYS Simplorer is another software package from ANSYS [27]. It is an integrated and multi domain platform to perform analysis on complex technical systems [27]. It allows to accurately and instantly design complex power electronic and electrically controlled system [28]. It can be used to develop circuits , inverters and control systems to simulate problems relating but not limited to electro-mechanical, electromagnetic, power, automotive, industrial automation,e.t.c [27][28]. The comprehensive tool provides accurate and reliable results. Simplorer is a unique simulator that can dynamically interact with other ANSYS application like Maxwell, Q3D and also with a third party simulator like MATLAB Simulink and Mathcad [27]. Data is seamlessly transferable from one platform to another allowing to solve complex and modular simulation problems.

4.2.1 Cosimulation

As mentioned earlier, Maxwell is an interactive softwage packages that uses FEA to solve 2D or 3D electromagnetic problem. In order to analyze the problem, Maxwell specifies the properties of the materials, excitation for device and appropriate geometry of the model [29]. When a Transient cosimulation Component sub circuit is used in a Simplorer platform, Maxwell 2D or 3D is able to exchange data during each simulation time step [29]. This is called transient cosimulation [29].

Maxwell 2D and 3D Transient solvers uses circuit equations into the finite element system of equations. It uses loop form of circuit equations whereas Simplorer used a nodal form of circuit equations [29]. In the end of each time step, Simploer creases a Norton equivalent of the drive circuit in the coupling pins between the Maxwell component and the rest of the system and converts it to a loop matrix to solve the finite element equations and provides a Thevenin-equivalent for the next time step [29].

In order to perform the transient analysis, the proposed motor required a drive system to operate. The drive system was created using Simplorer and cosimulation was carried out between Maxwell 3D model of the proposed motor with the drive unit built in Simplorer.

Chapter 5

Magentostatic Simulation

At first, magentostatic simulation was carried out in both the motors to analyze their performances. Magnetostatic is the study of magnetic fields in systems where the currents are steady [22]. We should be aware that magneto statics is only a good approximation even when the currents are not static as long as the currents do not alternate and rapidly constant current is provided. It should be noted that the motion of the motor was not involved in magnetostatic simulation instead a single phase was excited and the motor was rotated 2° for a complete 360°. This process was repeated for all three phases and the results were combined to achieve the final result of the motor for 360° with all three phases. The following bullet point outlines and summarizes the overview of Magentostatic analysis [22]:

- Magnetostatic analysis computes static magnetic fields.
- All objects (rotor in our case) are in stationary position.
- Magnetic field (H) is the quantity solved by magnetostatic analysis.
- Current density (J) and magnetic flux density (B) are automatically calculated from the magnetic field (H).
- Torques, inductances and forces can be calculated from the basic field quantities mentioned above.

This chapter presents the results of torque, inductance and force on both motors which are as follows.

5.1 Proposed AFSRM-Single layer Simulation

5.1.1 Single layer single phase excitation

Initially only one layer was used for simulation. A current of 2150A-Turns is chosen for simulation with 115 turns per winding giving current flowing through the winding to be 19A. If a voltage source with 650 V DC output is used to run this motor capable of supplying the current needed the power delivered would be approximately 12.35 kW for each layer. At first only one phase (Phase A) is excited and torque developed at different rotor angle is analyzed. Figure below shows the torque at different angular position of rotor at the step size of 2°.

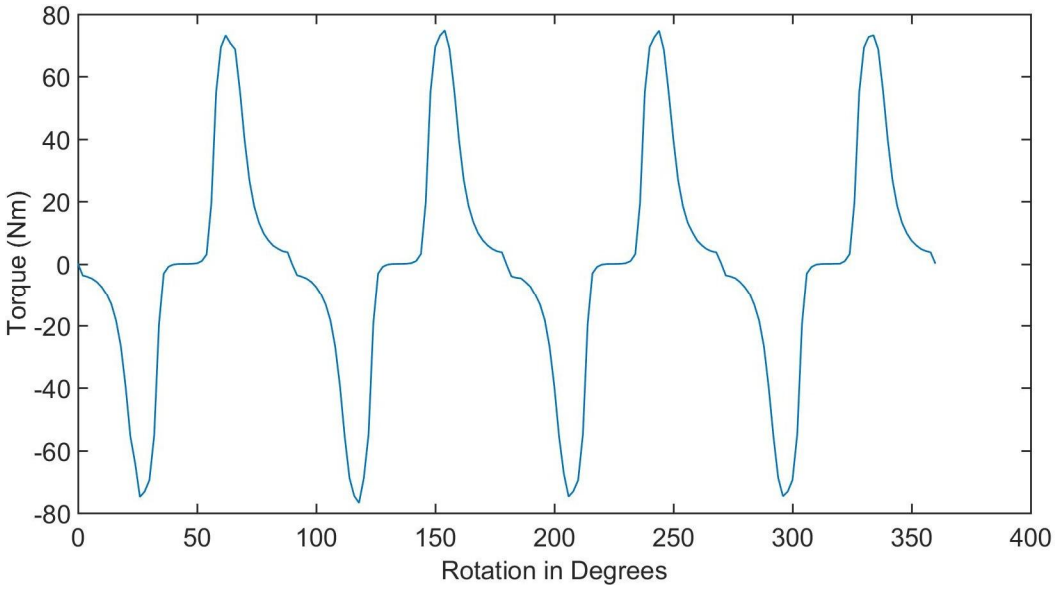

Figure 5.1: Torque developed at different rotor position with Phase A excited for one layer

The following figure shows the inductance at different rotor position for a complete 360° rotation.

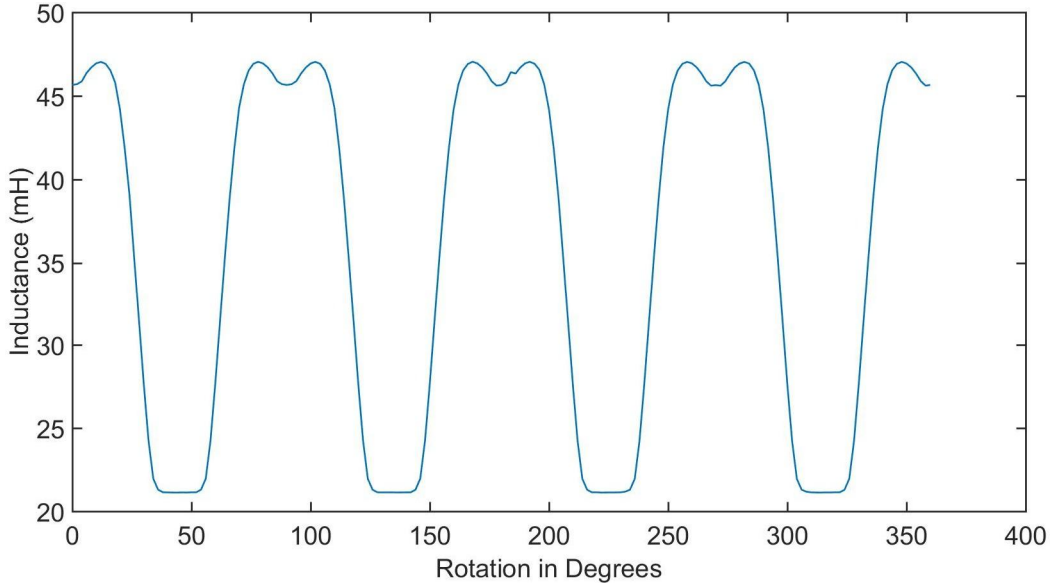

Figure 5.2: Inductance at different rotor position with Phase A excited for one layer

The following figure shows the radial force experienced by whole motor at different rotor angular position

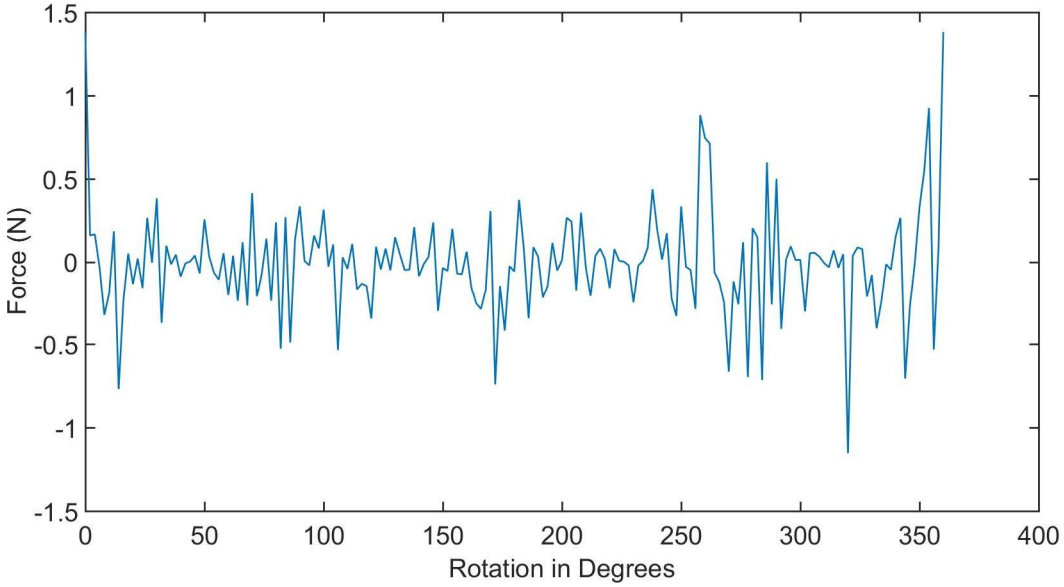

Figure 5.3: Radial Force experienced by the whole motor at different rotor position with Phase A excited for one layer

5.1.2 Single layer all phase sequentially excitation

Torque, inductance and radial force at different rotor position for all phase excited for single layer are shown in the following figures.

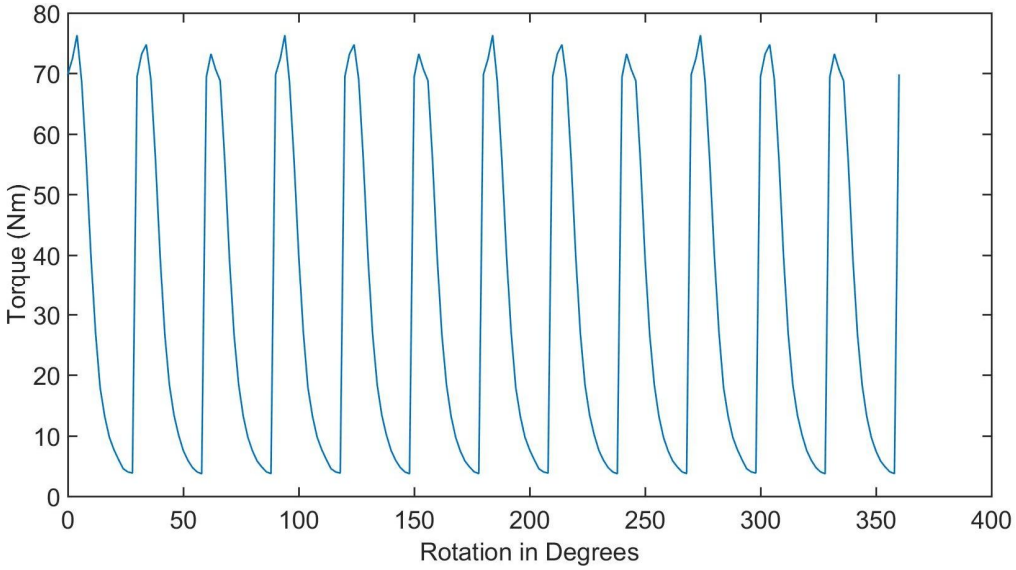

Figure 5.4: Torque at different rotor position with 3 Phase excitation for one layer

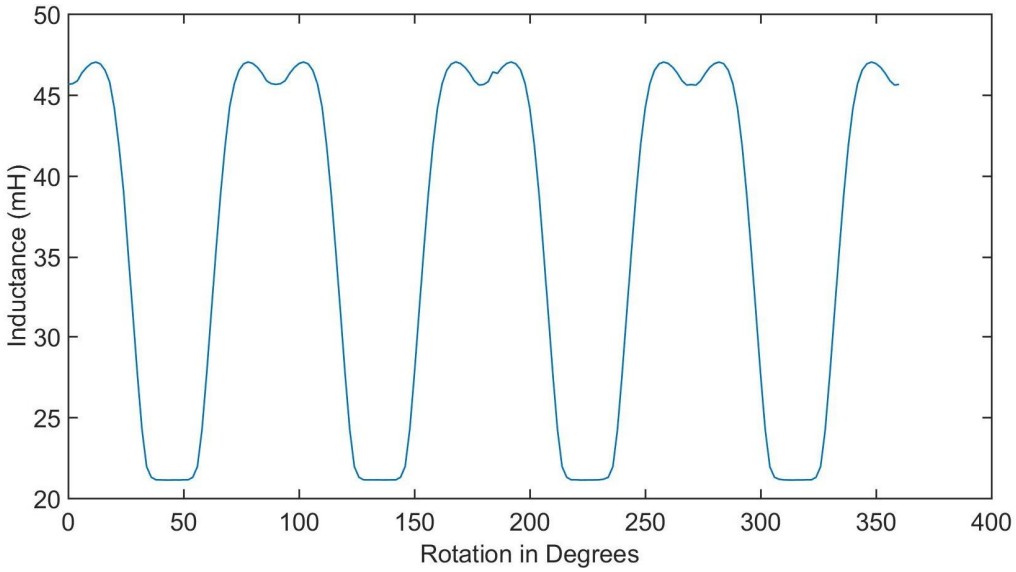

Figure 5.5: Inductance at different rotor position with 3 Phase excitation for one layer

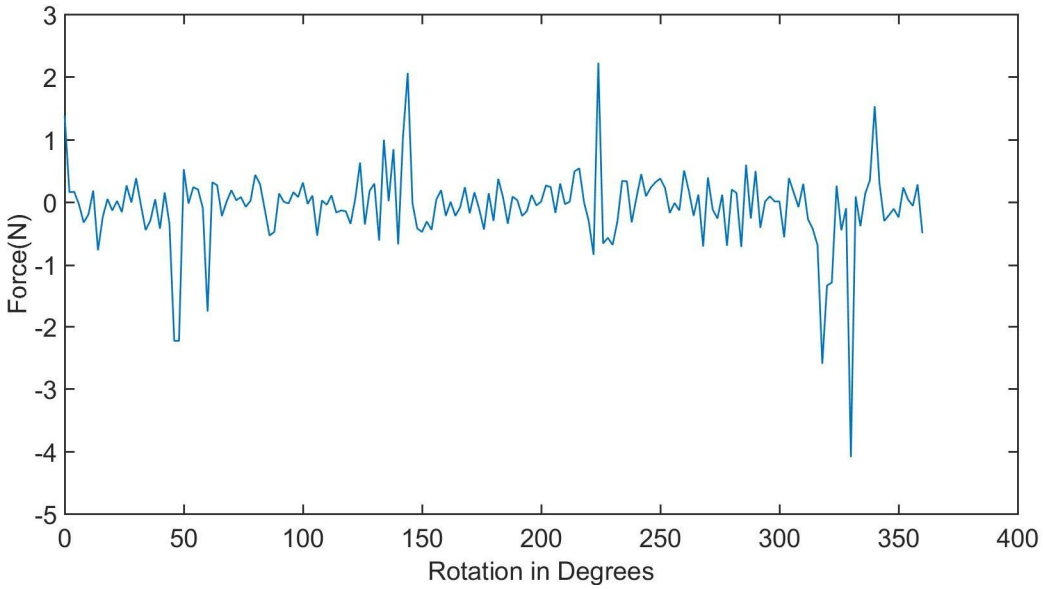

Figure 5.6: Radial force at different rotor position with 3 Phase excitation for one layer

5.1.3 Double layer single phase excitation

Phase A is excited in the first layer (bottom layer) with the current of 19.23A and 115 winding turns and Phase B is excited in the second layer (top layer) with the current of 19.23A and 115 winding turns. Figure below shows the torque at different angular position of rotor at the step size of 2°.

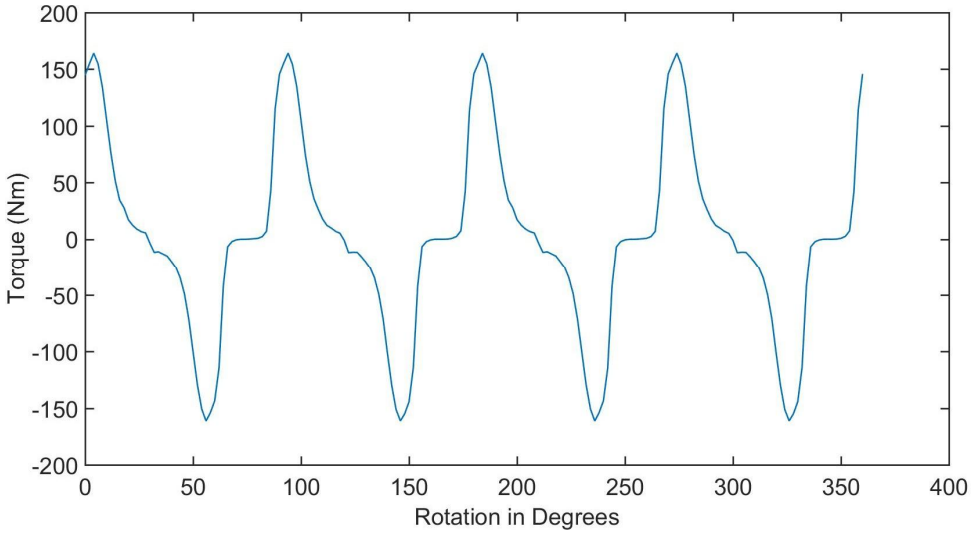

Figure 5.7: Torque developed at different rotor position with Phase A excited for double layer

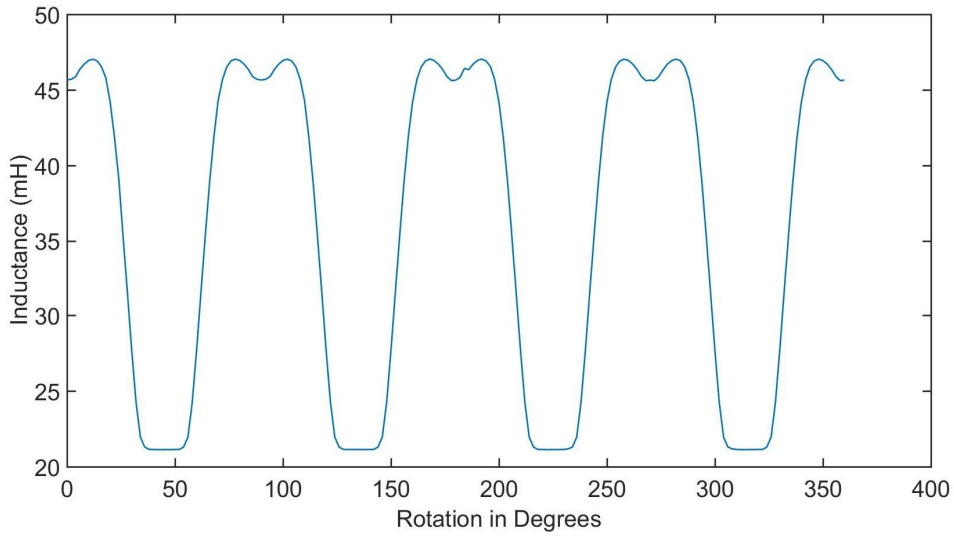

Figure 5.8: Inductance at different rotor position with Phase A excited for double layer

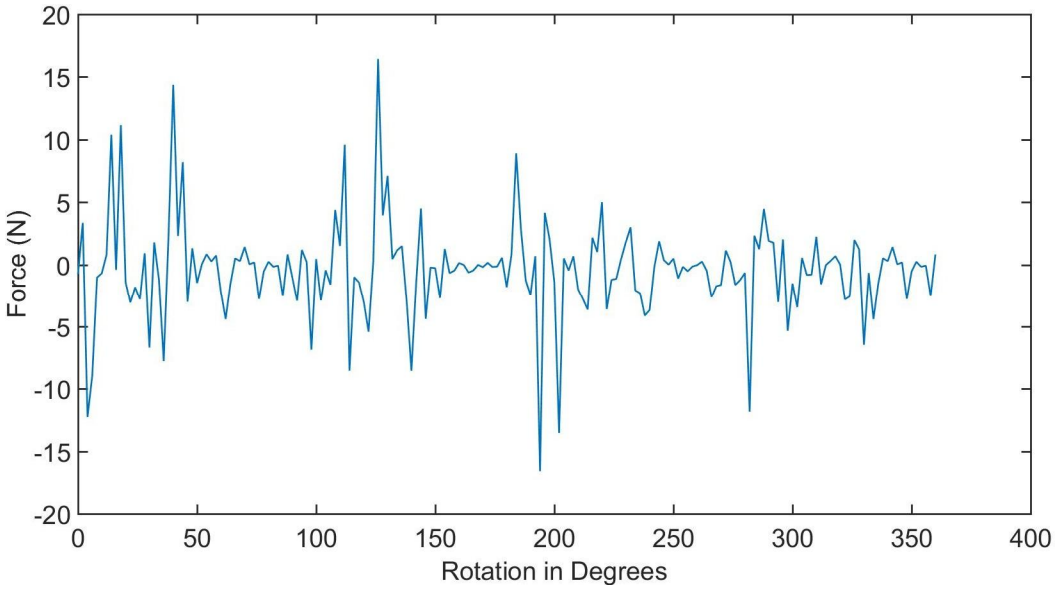

Figure 5.9: Radial Force experienced by the whole motor at different rotor position with Phase A excited for double layer

5.1.4 Double layer all phase sequentially excitation

Torque, inductance and radial force at different rotor position for all phase excited for double layer are shown in the following figures.

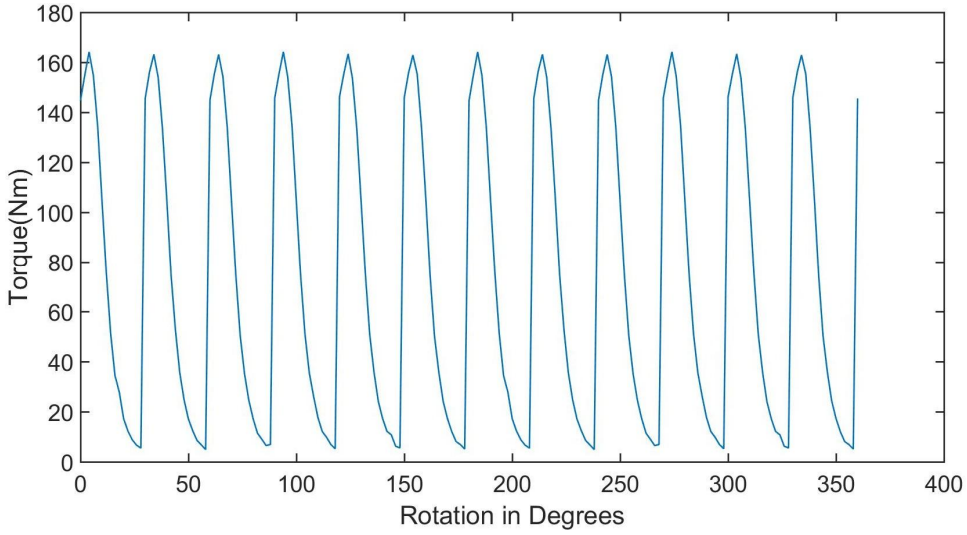

Figure 5.10: Torque at different rotor position with 3 Phase excitation for double layer

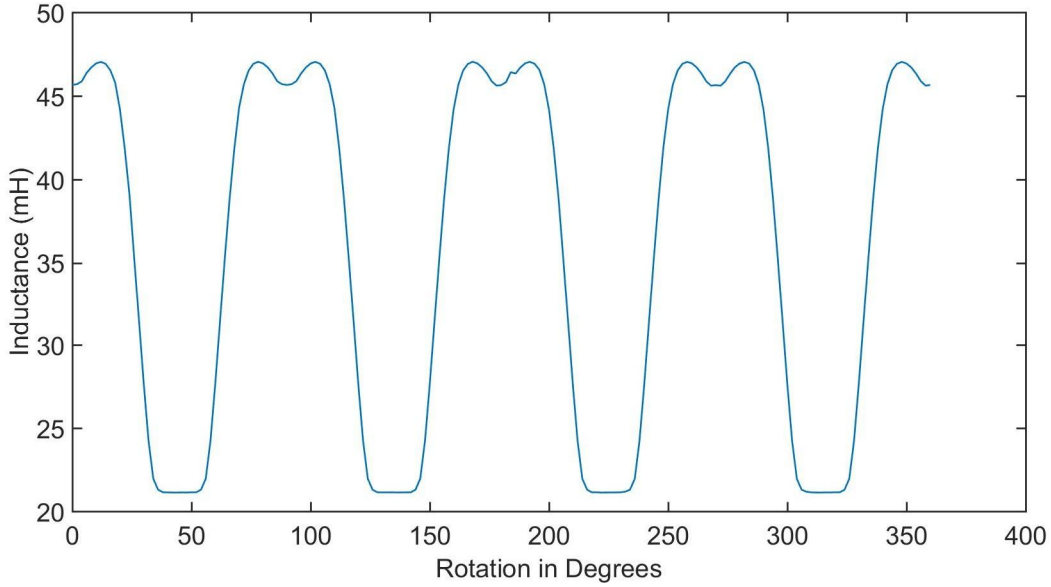

Figure 5.11: Inductance at different rotor position with 3 Phase excitation for double layer

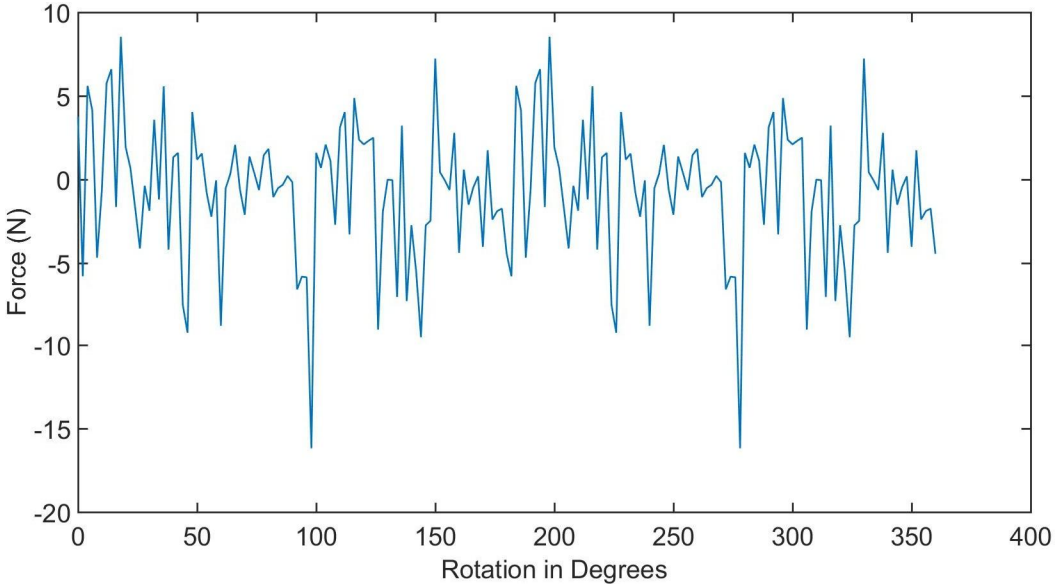

Figure 5.12: Radial force at different rotor position with 3 Phase excitation for double layer

5.1.5 Four layer single phase excitation

Phase A is excited in the first layer (bottom layer) with the current of 19.23A and 115 winding turns and Phase B is excited in the second layer (top layer) with the current of 19.23A and 115 winding turns and the same is done for the top two layers where 3rd layer is same as 1st layerand

4th layer is same as 2nd layer. Figure below shows the torque at different angular position of rotor at the step size of 2°.

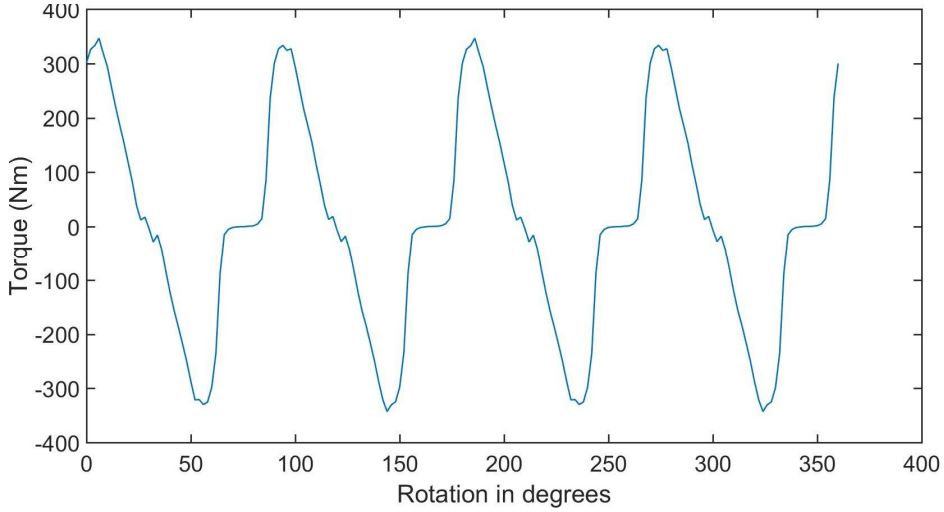

Figure 5.13: Torque developed at different rotor position with Phase A excited for four layer

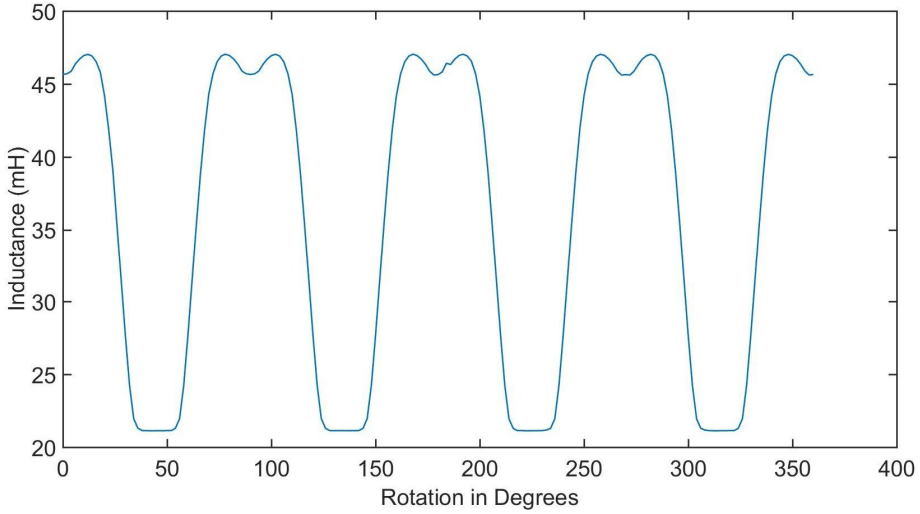

Figure 5.14: Inductance at different rotor position with Phase A excited for four layer

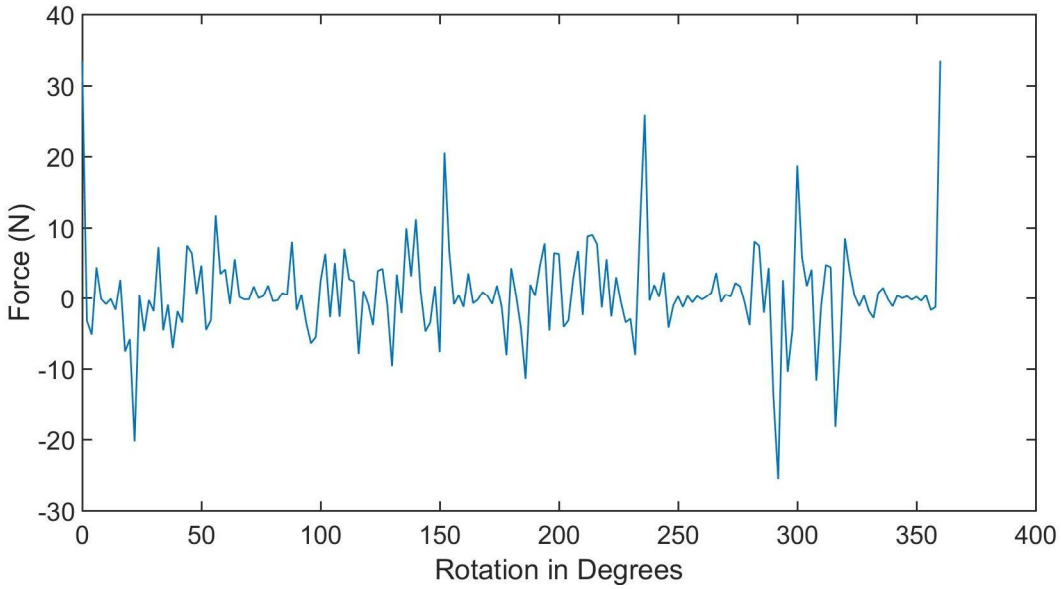

Figure 5.15: Radial Force experienced by the whole motor at different rotor position with Phase A excited for four layer

5.1.6 Four layer all phase sequentially excitation

Torque, inductance and radial force at different rotor position for all phase excited for four layers are shown in the following figures.

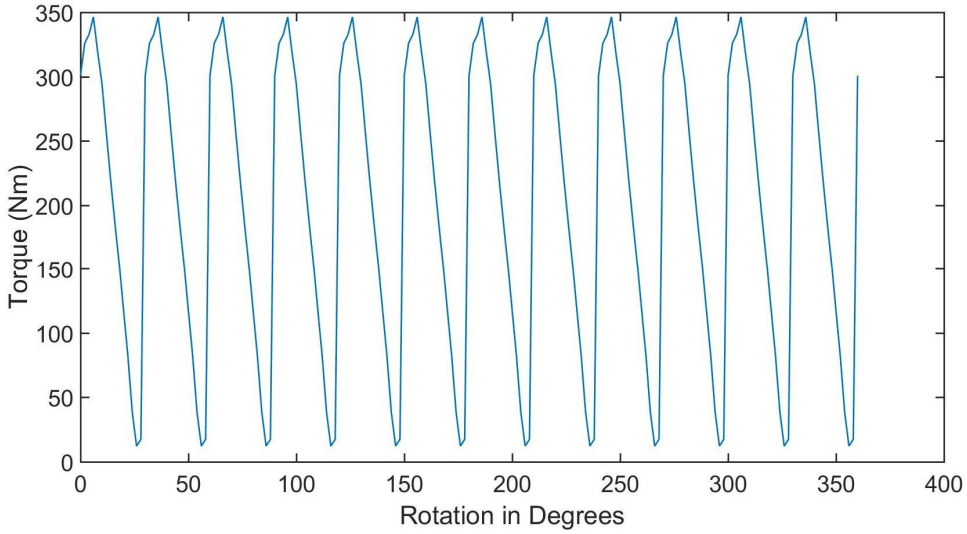

Figure 5.16: Torque at different rotor position with 3 Phase excitation for four layer

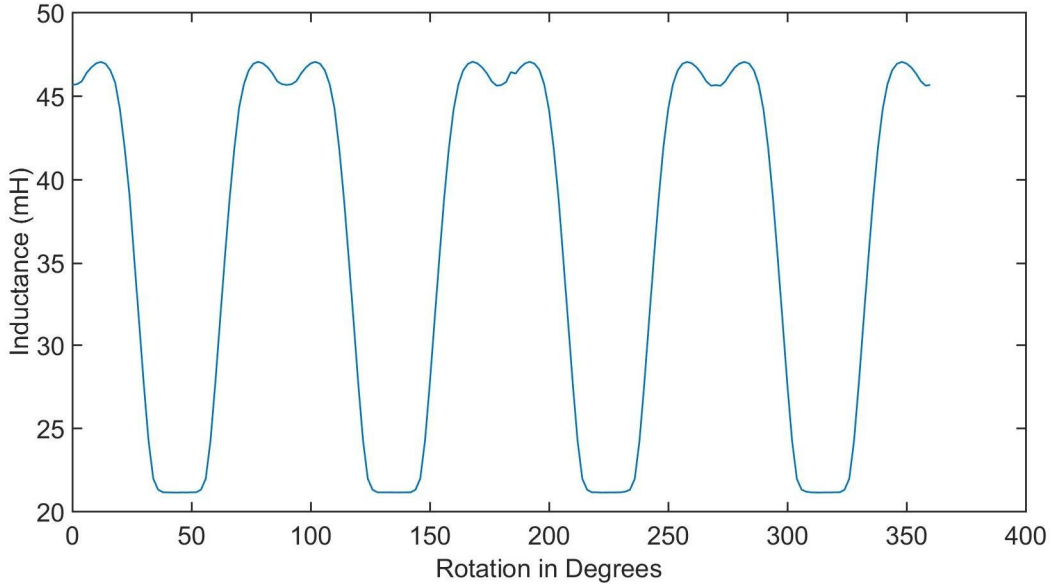

Figure 5.17: Inductance at different rotor position with 3 Phase excitation for four layer

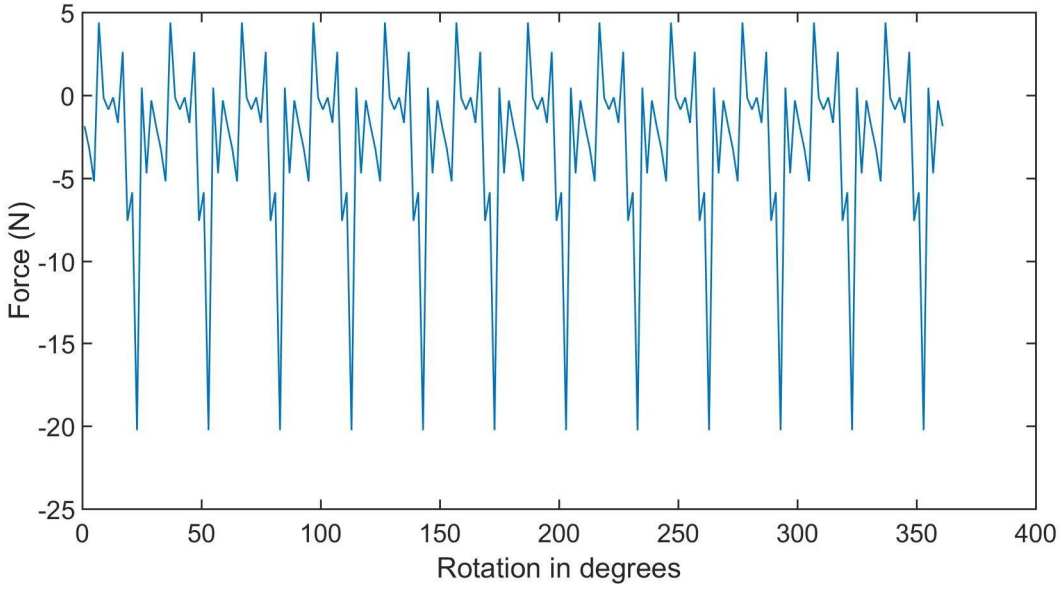

Figure 5.18: Radial force at different rotor position with 3 Phase excitation for four layer

5.2 Torque Comparison

The magnetostatic torque profile of the proposed motor when one, two and all four are excited are shown below. As observed, the torque value is proportional to the number of excited disks.

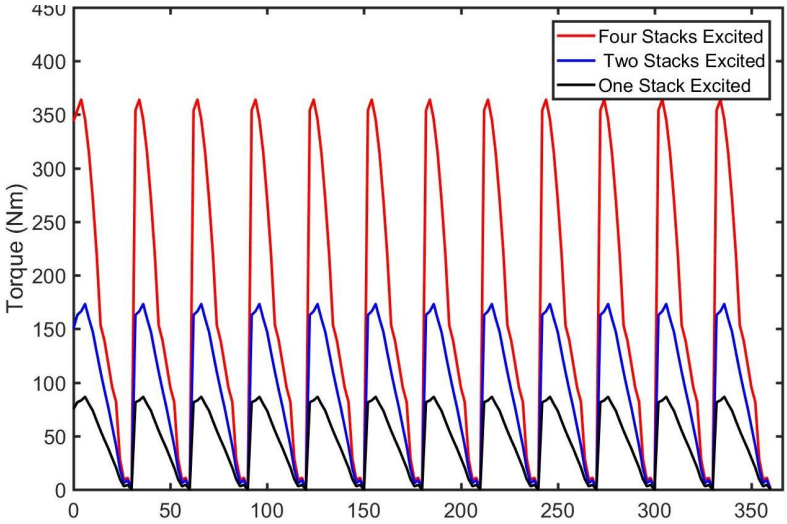

Figure 5.19: Characteristic of motor torque of proposed modular motor with 4 layers excitation

5.3 Conventional AFSRM Simulation

Torque, inductance and radial force at different rotor position for all phase excited for the conventional AFSRM are shown in the following figures.

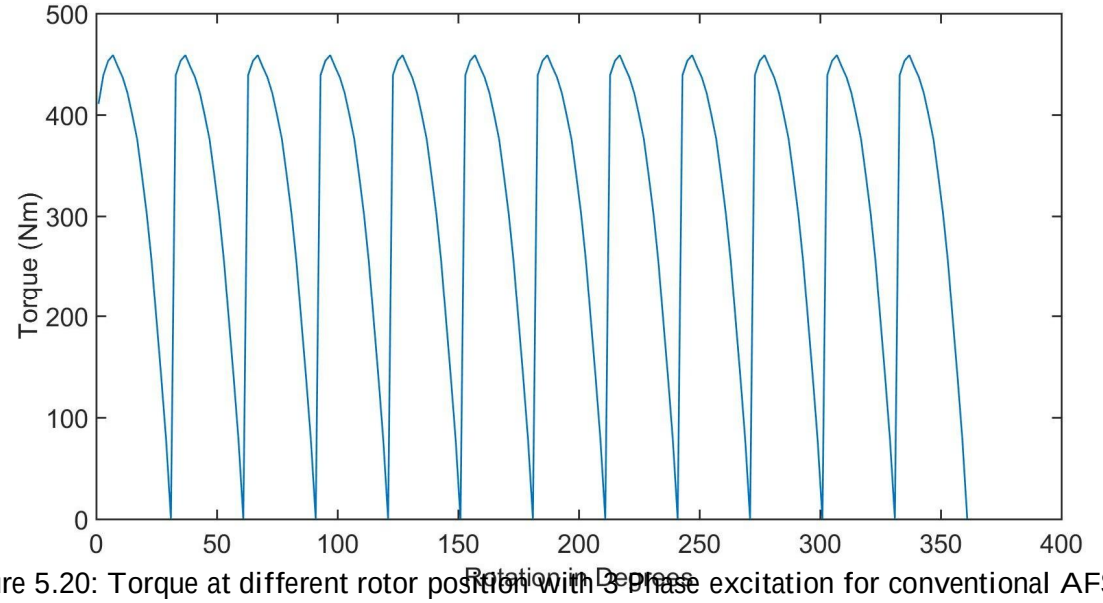

Figure 5.20: Torque at different rotor position with 3 Phase excitation for conventional AFSRM

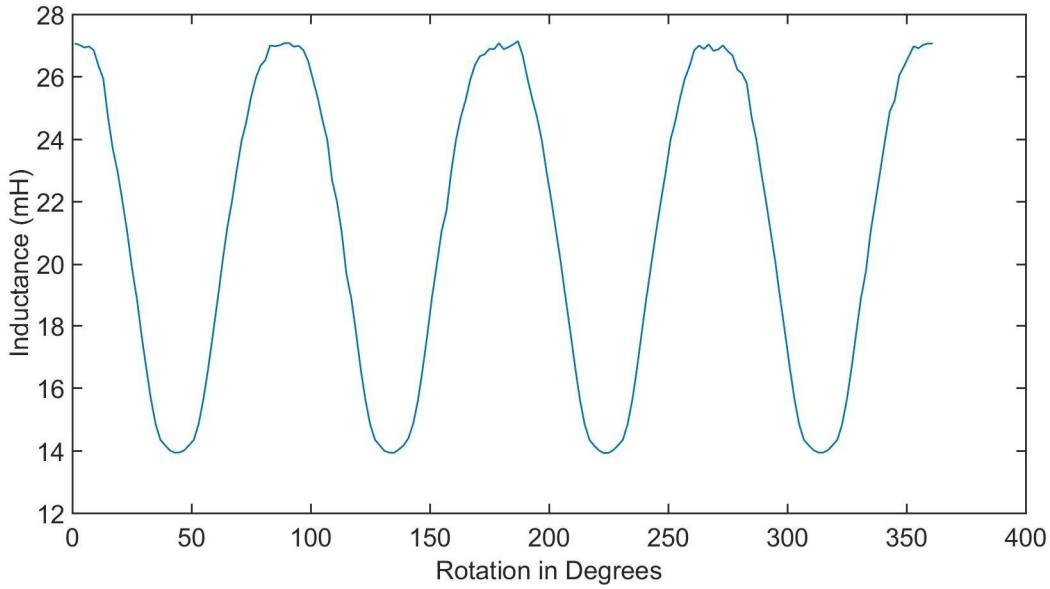

Figure 5.21: Inductance at different rotor position with 3 Phase excitation for conventional AFSRM

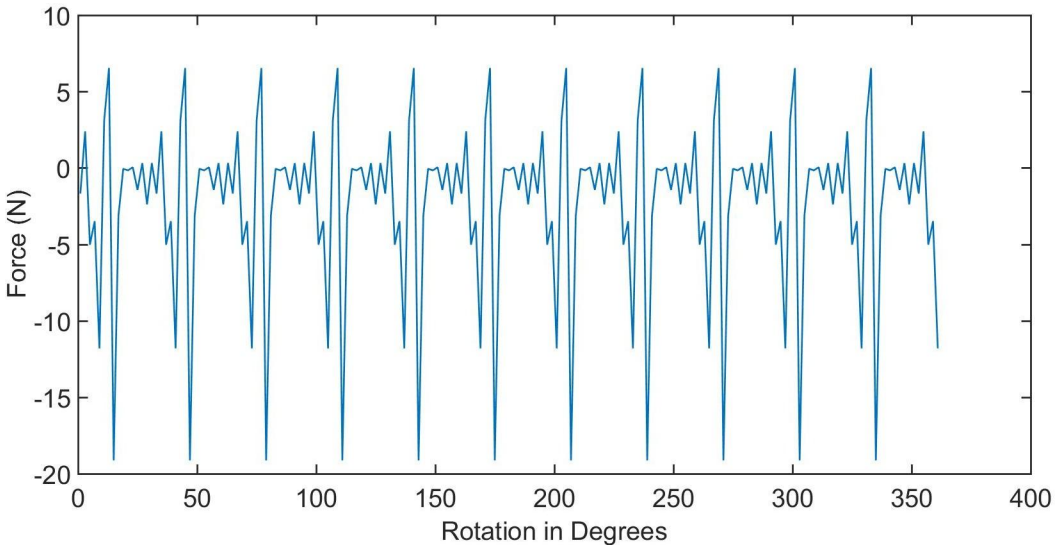

Figure 5.22: Radial force at different rotor position with 3 Phase excitation for conventional AF-SRM

5.4 Comparison between proposed four stack AFSRM and conventional stack motor

As mentioned earlier, one stack motor of 50kW was also simulated to compare the results to verify the need of four layers of 12.5kW motors (12.5kW*4=50kW). A single layer AFSRM has 4 times the stator width, stator tooth, rotor width, rotor tooth, number of turns of wire and excitation current than that of a individual single layer motor used in four layer AFSRM above. The stator and rotor diameter is same as the four layer motor and the height of both the motors are the same. The following table summarizes the comparison between a four- layer AFSRM and a single layer on the basis of maximum force on x-direction, maximun torque, ohmic losses and torque ripple that was obtained from FEM simulation in Ansys Maxwell.

Table 5.1: Magnetostatic results comparison for proposed motor and conventional motor

Motor Type	Max Torque (Nm)	Torque ripple (%)	Ohmic Loss (W) (FEM)
Proposed four layer	346.9	150	130
Conventional	350	130	640

Comparison between a four- layer AFSRM and a convnetional single layer

For torque ripple, following formula was used.

$$T_{ripple}(\%) = \frac{(T_{max} - T_{min})}{2 * T_{avg}} X100 \quad (5.1)$$

where T_{max}, T_{min} and T_{avg} are the maximum torque, minimum torque and average torque. From the above table it can be seen that even though the maximum torque generated from one stack motor is half than the four layered motor, the ohmic losses in one stack motor is about four times higher than that of the four layer motor. This makes a four layer axial flux switch reluctance motor to have higher torque output but than one stack motor given the same power and voltage parameters.

Magnetostatic is only useful to study steady state response at different rotor positions which is good to study steady state torque and inductance. Overall, although results were as expected, the simulations did not include a drive system, instantaneous switching & actual motion of the motor. Therefore, we saw a need for transient analysis which is presented in the following chapter.

Chapter 6

Transient Simulation

For transient analysis, we need to design a drive unit in that would be able to do the switching at every 30 degrees shift in rotor. It also needs a feedback system to get the accurate position of the rotor to be able to do switching of phases accurately. Moreover, our current limit should not be exceeded as it would not give us a realistic scenario. Therefore, we need a drive system that senses the rotor position actively as well as controls the drawing of current.

6.1 Design of Drive System

Following figure illustrates the drive/control unit adopted for the transient analysis [30]. It consists of a full bridge power converter fed from the 650V DC source along with twelve diodes to provide return paths for the current. The drive unit is controlled by the current hysteresis and voltage Pulse Width Modulation (PWM) method.

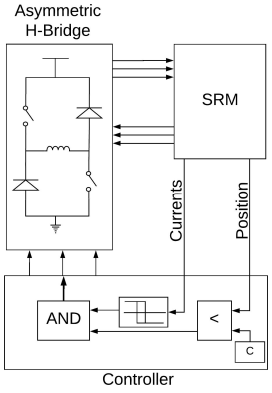

Figure 6.1: Axial Flux Switched Reluctance motor drive system.

The controller provides the switching commands based on the rotor position. There are two methods of energizing the phase winding of the motor. One is the voltage control and the other one is the hysteresis current control [30]. In the voltage control, the voltage is applied through the

converter when the slope of inductance is positive and is removed before the slope of inductance is negative to avoid negative torque [30]. This method is applied using a 3-phase asymmetric H-Bridge converter. Hysteresis current control is used to keep the current at the rated value.

6.2 Drive System Using Ansys Simplorer

The motor is modeled in a 3-D FEA software package and is co-simulated with the hysteresis current control unit developed in the electronic circuit design software tool. The dynamic link provides the ability to let the circuit design tool vary variables in the FEA motor model and to let FEA model solve the new design point and provide the solution back to the circuit design tool for co-simulation [22]. A diagram of data flow from each simulation mode in the co-simulation is shown in figure below.

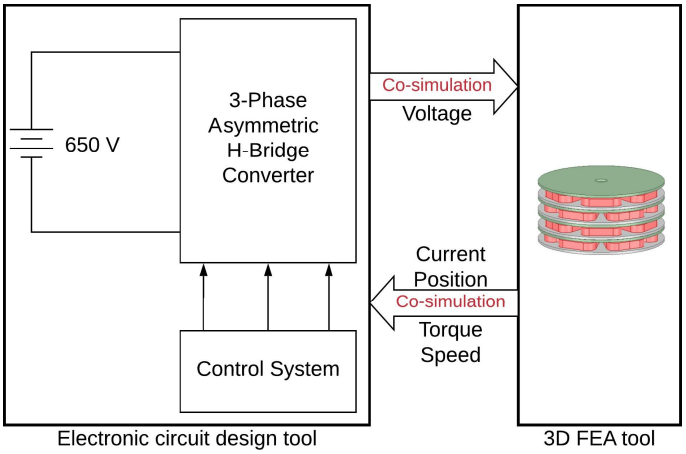

Figure 6.2: Data flow between FEA software and the circuit design tool.

6.3 Current Profile

The motor is supplied by 650 VDC and rotated with the speed of 360 rpm. The hysteresis current control is applied to excite the phase windings. The related per phase current profile for the proposed motor and the conventional motor is shown in Figs. 6.3 and 6.4 respectively. As seen, the value of the phase current is approximately 19 A in the proposed motor and 76 A in the conventional motor. This could significantly decrease the stator winding ohmic loss. Based on following equations on ohmic loss, the ohmic loss is proportional to the square of the current.

Although, the overall wiring length in the proposed 4-layer structure is quadruple of that in the conventional 1-layer structure, the stator current is four times less.

$$P_{cop} = R * I^2 \tag{6.1}$$

$$P_{cop.new} = 4 * R * (\frac{I}{4})^2 \tag{6.2}$$

In rated current 76.9A, ohmic losses ratio is obtained as:

$$\frac{P_{cop}}{P_{cop.new}} = 4 \tag{6.3}$$

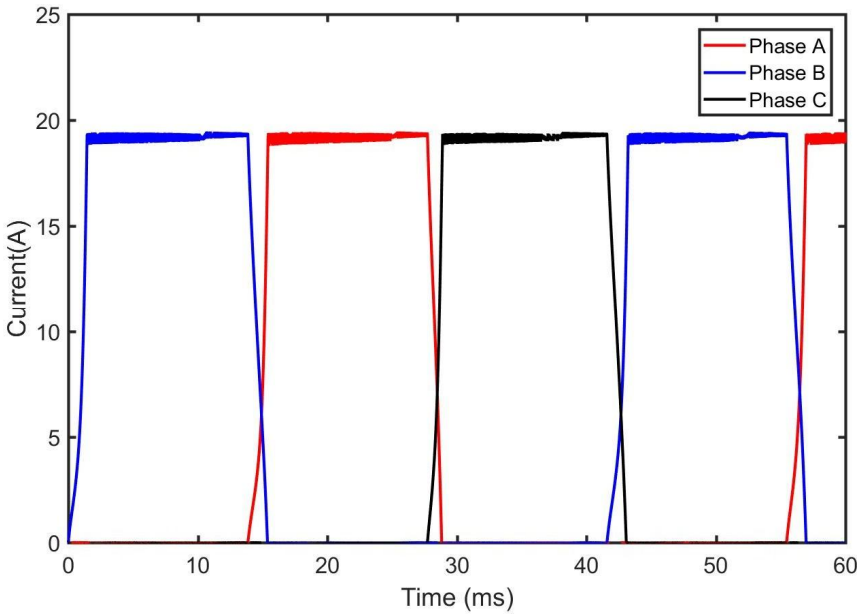

Figure 6.3: The profile of the phase current in the proposed motor.

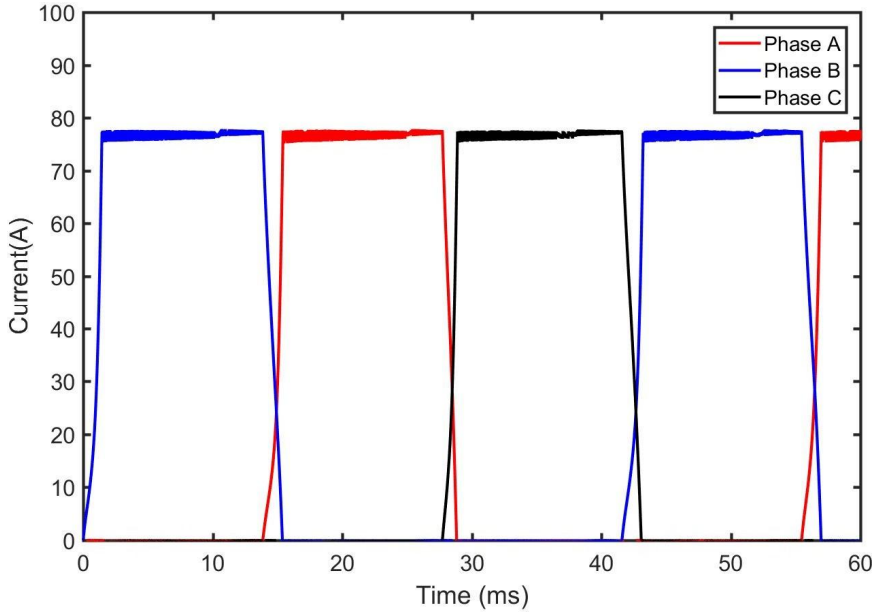

Figure 6.4: The profile of the phase current in the conventional motor.

6.4 Torque Profile

The profile of the transient torque of the proposed modular structure is simulated and plotted against the results of the conventional motor in the following figure.

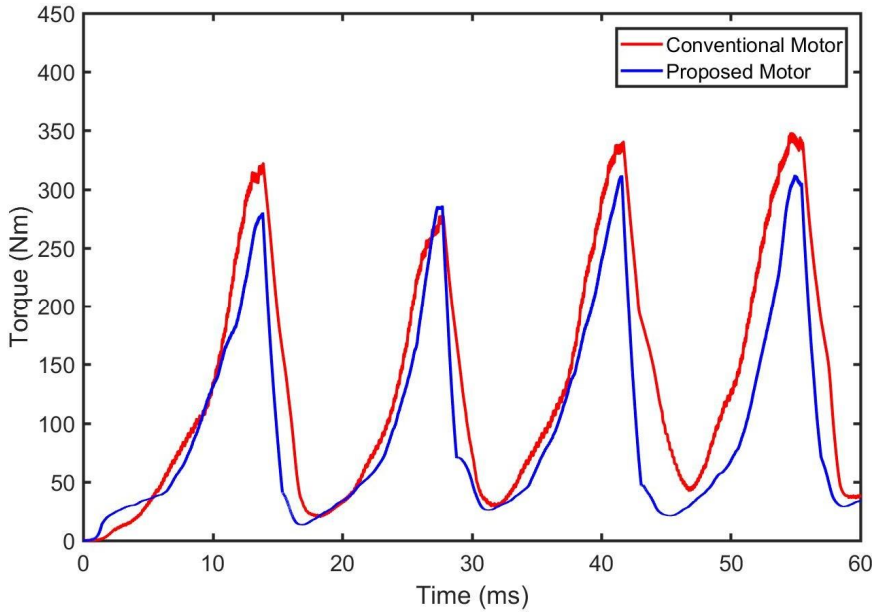

Figure 6.5: Transient torque profile of the proposed motor Vs the conventional motor.

Table 6.1: Transient torque results comparison for proposed motor and conventional motor

Motor Type	Avg. Torque (Nm)	Torque ripple (%)
Proposed four layer	96	120.8
Conventional	112	137.5

Comparison between a four- layer AFSRM and a conventional single layer

The torque ripple and average torque output for both proposed and conventional motor are presented in table above.

6.5 Radial Force

To assess the effectiveness of the proposed design in reducing unwanted radial forces, the radial force of the proposed four layer modular design is plotted against the conventional single stack motor in figure below. To conduct a fair comparison, the motor data (e.g. dimensions, rated power, voltage. etc) are selected to be equal in both motors.

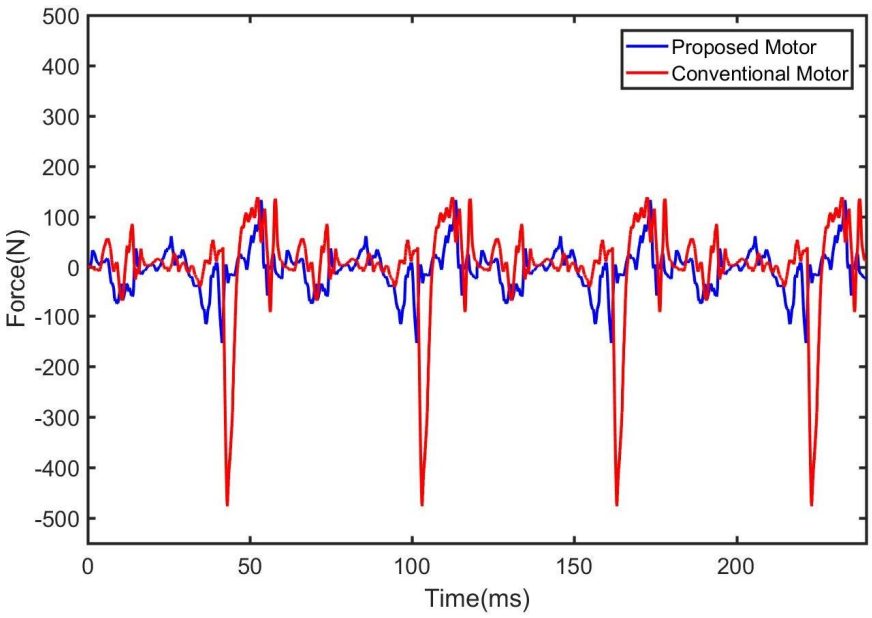

Figure 6.6: Radial force of the proposed motor Vs the conventional motor.

The torque ripple and average torque output for both proposed and conventional motor are presented in table below.

Table 6.2: Transient radial force results comparison for proposed motor and conventional motor

Type	Avg. Force (N)	Standard Deviation(%)
Conventional	5.92	57.38
Proposed	4.2	21.1

Comparison between a four- layer AFSRM and a conventional single layer

Chapter 7

Conclusion & Future Works

In this study, a new modular structure for AFSRMs based on four stator/rotor disks is proposed and the proposed motor shows higher reliability, lower ohmic winding loss, lower torque ripple & less radial force. According to the FEA analysis results, the torque ripple was reduced by 17% and the radial force by 33.2 %. The proposed structure distributes radial forces and torque strokes along the axial length of the motor, effectively reducing the vibration. The following are the scope of the future works for this research:

- Vibration analysis can be done in the existing structure to ensure reduced vibration in the motor.
- Further improvement can be done by optimizing motor drive unit
- Half-stepping can be used to minimize torque ripple and radial forces
- Development of prototype to test the design.

Bibliography

[1] Wikimedia Commons, " Switched-reluctance-motor-characteristics-work-principles-t.jpg, " 2017. [Online; accessed 07-June-2019].

[2] D. Son, D. Lee, and J. Ahn, " Design and analysis of double stator axial field type srm, " in *2017 IEEE Transportation Electrification Conference and Expo, Asia-Pacific (ITEC Asia-Pacific)*, pp. 1 – 6, Aug 2017.

[3] J. A. Makwana, P. Agarwal, and S. P. Srivastava, " Novel simulation approach to analyses the performance of in-wheel srm for an electrical vehicle, " in *2011 International Conference on Energy, Automation and Signal*, pp. 1 – 5, Dec 2011.

[4] M. Divandari, B. Rezaie, and B. Askari-Ziarati, " Torque estimation of sensorless srm drive using adaptive-fuzzy logic control, " in *2016 IEEE NW Russia Young Researchers in Electrical and Electronic Engineering Conference (EIConRusNW)*, pp. 542 – 546, Feb 2016.

[5] R.Krishnan, *Switched Reluctance Motor Drives*, vol. 4 of *10*. 2000 N.W. Corporate Blvd., Boca Raton, Florida 33431: CRC press, 7 2001.

[6] M. Aydin, M. Gulec, Y. Demir, B. Akyuz, and E. Yolacan, " Design and validation of a 24-pole coreless axial flux permanent magnet motor for a solar powered vehicle, " in *2016 XXII International Conference on Electrical Machines (ICEM)*, pp. 1493 – 1498, Sep. 2016.

[7] B. Fahimi, A. Emadi, and R. B. Sepe, " A switched reluctance machine-based starter/alternator for more electric cars, " *IEEE Transactions on Energy Conversion*, vol. 19, pp. 116 – 124, March 2004.

[8] B. Poudel, E. Amiri, and P. Rastgoufard, " Design and analysis of line start synchronous reluctance motor with dual saliency, " in *2018 IEEE Transportation Electrification Conference and Expo (ITEC)*, pp. 385 – 388, June 2018.

[9] N. Neupane, " Comparison of switched reluctance motor and double stator switched reluctance motor, " Master ' s thesis, University of New Orleans, New Orleans, LA, 12 2018. An optional note.

[10] E. Amiri, B. Poudel, A. D. Aliabad, F. Ghoroghchian, and O. Dobzhanskyi, " The emergence of dual pole line start synchronous motors, " in *2018 IEEE Energy Conversion Congress and Exposition (ECCE)*, pp. 1656 – 1660, 2018.

[11] R. Madhavan and B. G. Fernandes, " Performance improvement in the axial flux-segmented rotor-switched reluctance motor," *IEEE Transactions on Energy Conversion*, vol. 29, pp. 641 – 651, Sep. 2014.

[12] K. Sitapati and R. Krishnan, " Performance comparisons of radial and axial field, permanent-magnet, brushless machines, " *IEEE Transactions on Industry Applications*, vol. 37, pp. 1219 – 1226, Sep. 2001.

[13] B. Poudel and E. Amiri, " Aggregate model of single phase induction motors, " 05 2019.

[14] T. Miller, *Switched Reluctance Motors and Their Control*, vol. 1 of *1*. Oxford,U.K.: Oxford University press, 7 1993.

[15] S. Smaka, . Mašić, M. Ćosović, and I. Salihbegović in *The XIX International Conference on Electrical Machines - ICEM 2010*.

[16] B. Poudel, E. Amiri, and D. Charalampidis, " Design improvement of dual pole synchronous reluctance motor, " in *2018 IEEE Energy Conversion Congress and Exposition (ECCE)*, pp. 5403 – 5407, Sep. 2018.

[17] C. Sahin, A. E. Amac, M. Karacor, and A. Emadi, " Reducing torque ripple of switched reluctance machines by relocation of rotor moulding clinches, " *IET Electric Power Applications*, vol. 6, pp. 753 – 760, November 2012.

[18] F. Sahin, H. B. Ertan, and K. Leblebicioglu, " Optimum geometry for torque ripple minimization of switched reluctance motors, " *IEEE Transactions on Energy Conversion*, vol. 15, pp. 30 – 39, March 2000.

[19] J.F.Tsai and Y. P. Chen, " Design and performance analysis of an axial-flux disk-type switched relucatnce motor for hybrid scooters, " *JSME International Journal*, vol. 34, pp. 882 – 889, March 2006.

[20] C. Hua, P. Xu, Q. Ma, and W. Ye, " Performance analysis of switched reluctance motor based on maxwell and simplorer, " in *2017 Chinese Automation Congress (CAC)*, pp. 6510 – 6515, Oct 2017.

[21] X. Han, D. Jiang, T. Zou, R. Qu, and K. Yang, " Two-segment three-phase pmsm drive with carrier phase-shift pwm for torque ripple and vibration reduction, " *IEEE Transactions on Power Electronics*, vol. 34, pp. 588 – 599, Jan 2019.

[22] A. MAXWELL, " Maxwell online help. " Help Guide, 2018.

[23] A. MAXWELL, " Maxwell rmxpert online help. " Help Guide, 2017.

[24] , " Maxwell equations, " 2017. [Online; accessed 07-June-2019].

[25] Ansoft, " Maxwell 3d, " 2005. [Online; accessed 07-June-2019].

[26] ANSYS Inc, " Ansys maxwell 3d user ' s guide, " 2010. [Online; accessed 17-June-2019].

[27] Ansoft, " Simplorer the multi domain simulator, " 2002. [Online; accessed 12-May-2019].

[28] ANSYS Inc, " Simplorer, " 2011. [Online; accessed 12-June-2019].

[29] ANSYS, *Simplorer Online Help*. ANSYS.

[30] E. Elhomdy, G. Li, J. Liu, S. Bukhari, and W.-P. Cao, " Design and experimental verification of a 72/48 switched reluctance motor for low-speed direct-drive mining applications, " *Energies*, vol. 11, p. 192, Jan 2018.

Appendix

Matlab Code

```
close all; clear; clc;
font=16;
linewidth=2;
T= xlsread('a.xlsx');
x=T(:,1);
for_4= T(:,2);
for_1= T(:,3);

figure();
% subplot(3,1,1);
plot(x,for_4,'k','LineWidth',linewidth);
 hold on;
% plot(x,tor_2,'b','LineWidth',linewidth);
 plot(x,for_1,'r','LineWidth',linewidth);
ylim([-50,75]);
xlim([0,366]);
xlabel('Rotation (degrees)','FontSize',font);
ylabel('Force (N)','FontSize',font);
legend('Proposed Motor','Conventional Motor');
set(gca,'FontSize',font,'LineWidth',linewidth);

set(gcf,'units','normalized','outerposition',[0 0 0.5 0.65])
saveas(gcf,  'Radial Force.jpg');
%close;
```

```
close all; clear; clc;
font=16;
linewidth=2;
```

```
T = xlsread('Proposed 4 stack Inductance.xlsx');

prompt = 'What is the aligned inductance? ';
La = input(prompt)
prompt= 'What is the unaligned inductance? ';
Lu=input(prompt)
prompt= 'What is the midway inductance? ';
Lm=input(prompt);
 Nr=input('How many poles are there in the rotor? ');
L0 = 0.5*(0.5*(La+Lu)+Lm);
 L1=0.5*(La-Lu);
L2 = 0.5*(0.5*(La+Lu)-Lm);


 for i=1:1:360

      in(i)=(L0+L1*cosd(4*i)+L2*cosd(8*i)) %% accounts for inductance of
          both stator poles

%     D(i) = -L1*sin(4*i)*8-L2*sin(8*i)*16   %% accounts for derivative
      of both stator pole

end

% ind=transpose(ind)
% plot(b,a);
% hold on
% plot(b,z)
% legend('mes','fem');
 in=in(1:2:end)
```

```
a_ind= in ;
r = 0:2:358;
x=T(:,1);
 f_ind= T(:,4);
 figure();
% subplot(3,1,1);
 plot(r,a_ind,'r','LineWidth',linewidth);
  hold on;
 plot(x,f_ind,'b','LineWidth',linewidth);


 ylim([15,50]);
 xlim([0,366]);
 xlabel('Rotation (degrees)','FontSize',font);
 ylabel('Inductance (mH)','FontSize',font);
 legend('Analytical','FEA');
 set(gca,'FontSize',font,'LineWidth',linewidth);
 set(gcf,'units','normalized','outerposition',[0 0 0.5 0.65])
 saveas(gcf,  'p Analytical Vs FEA Inductance.jpg');%close;
```

```
prompt = 'What is the aligned inductance?';
La = input(prompt)
prompt= 'What is the unaligned inductance?';
Lu=input(prompt)
prompt= 'What is the midway inductance?';
Lm=input(prompt);
 Nr=input('How many poles are there in the rotor? ');
L0 = 0.5*(0.5*(La+Lu)+Lm);
 L1=0.5*(La-Lu);
L2 = 0.5*(0.5*(La+Lu)-Lm);

```

```
12
13 for i=1:1:360
14
15       in(i)=(L0+L1*cosd(4*i)+L2*cosd(8*i)) %% accounts for inductance of
             both stator poles
16
17 %     D(i) = -L1*sin(4*i)*8-L2*sin(8*i)*16    %% accounts for derivative
       of both stator pole
18
19 end
20
21 % ind=transpose(ind)
22 % plot(b,a);
23 % hold on
24 % plot(b,z)
25 % legend('mes','fem');
26  in=in(1:2:end)
27   plot(r,in)
```

```
1  close all; clear; clc;
2  font=16;
3  linewidth=2;
4 T = xlsread('Conventional and Proposed Torque.xlsx');
5 x=T(:,1);
6  p_tor= T(:,2);
7  c_tor= T(:,3);
8  % tor_1=f_tor/4;
9  % tor_2=f_tor/2;
10  figure();
11 % subplot(3,1,1);
12  plot(x,p_tor,'b','LineWidth',linewidth);
```

```
 hold on;
plot(x,ctor,'r','LineWidth',linewidth);
%plot(x,tor1,'k','LineWidth',linewidth);
ylim([0,500]);
xlim([0,366]);
xlabel('Rotation (degrees)','FontSize',font);
ylabel('Torque (Nm)','FontSize',font);

legend('Proposed Motor','Conventional Motor', 'Location','NorthEast');
set(gca,'FontSize',font,'LineWidth',linewidth);

set(gcf,'units','normalized','outerposition',[0 0 0.5 0.65])
saveas(gcf, 'Conventional Vs Proposed Torque.jpg');
%close;
```

```
close all; clear; clc;
font=16;
linewidth=2;
T=xlsread('Proposed 4stack Torque.xlsx');
x=T(:,1);
a_tor=T(:,2);
f_tor=T(:,3);
tor_1=f_tor/4;
tor_2=f_tor/2;
figure();
%subplot(3,1,1);
plot(x,ator,'r','LineWidth',linewidth);
 hold on;
plot(x,tor2,'b','LineWidth',linewidth);
plot(x,tor1,'k','LineWidth',linewidth);
ylim([0,450]);
```

```
xlim([0,366]);
xlabel('Rotation (degrees)','FontSize',font);
ylabel('Torque (Nm)','FontSize',font);
legend('Four Stacks Excited','Two Stacks Excited', 'One Stack Excited'
    ,'Location','NorthEast');
set(gca,'FontSize',font,'LineWidth',linewidth);
set(gcf,'units','normalized','outerposition',[0 0 0.5 0.65])
saveas(gcf, 'One Vs two Vs four layers.jpg');
%close;
```

```
close all; clear; clc;
font=16;
linewidth=2;
T= xlsread('switch.xlsx');
x=T(:,1);
sw_a= T(:,2);
sw_b= T(:,3);
sw_c=T(:,4);
sw_d= T(:,5);
sw_e= T(:,6);
sw_f=T(:,7);

figure();
subplot(2,1,1);
plot(x,sw_a,'r','LineWidth',linewidth);
 hold on;
plot(x,sw_b,'b','LineWidth',linewidth);
plot(x,sw_c,'k','LineWidth',linewidth);
ylim([0 2]);
yticks([0 1 2]);
xticks([0 30 60 90 120 150 180 210 240 270 300 330 360]);
```

```
%xlim([0,360]);
xlabel('Rotation (degrees)','FontSize',font);
ylabel('Switch State for Stator 1','FontSize',font);
legend('Phase A','Phase B','Phase C','Location','SouthEast');
set(gca,'FontSize',font,'LineWidth',linewidth);
subplot(2,1,2);
plot(x,swd,'r','LineWidth',linewidth);
  hold on;
plot(x,swe,'b','LineWidth',linewidth);
plot(x,swf,'k','LineWidth',linewidth);
ylim([0 2]);
yticks([0 1 2]);
xticks([0 30 60 90 120 150 180 210 240 270 300 330 360]);
xlabel('Rotation (degrees)','FontSize',font);
ylabel('Switch State for Stator 2','FontSize',font);
legend('Phase A','Phase B','Phase C','Location','SouthEast');
set(gca,'FontSize',font,'LineWidth',linewidth);
set(gcf,'units','normalized','outerposition',[0 0 0.5 0.65])
saveas(gcf,  'switching scheme.jpg');
%close;
```

```
close all; clear; clc;
font=16;
linewidth=2;
T=xlsread('Proposed 4stack Torque.xlsx');
x=T(:,1);
a_tor=T(:,2);
f_tor=T(:,3);
tor_1=f_tor/4;
tor_2=f_tor/2;
figure();
```

```
% subplot(3,1,1);
 plot(x,a_tor,'r','LineWidth',linewidth);
  hold on;
  plot(x,f_tor,'b','LineWidth',linewidth);
ylim([0,450]);
xlim([0,366]);
xlabel('Rotation (degrees)','FontSize',font);
ylabel('Torque (Nm)','FontSize',font);
legend('Analytical','FEA');
set(gca,'FontSize',font,'LineWidth',linewidth);
set(gcf,'units','normalized','outerposition',[0 0 0.5 0.65])
saveas(gcf,'Proposed Motor Analytical Vs FEA.jpg');
close;
```

```
close all; clear; clc;
font=16;
linewidth=2;
T = xlsread('Conventional Motor Torque.xlsx');
x=T(:,1);
 tor= T(:,2);
Q = xlsread('Proposed 4 stack Torque.xlsx');
y=Q(:,1);
 tor_4= Q(:,2);
% f_tor= T(:,3);
% tor_1=f_tor/4;
% tor_2=f_tor/2;
figure();
% subplot(3,1,1);
plot(x,tor,'r','LineWidth',linewidth);
  hold on;
  plot(y,tor_4,'b','LineWidth',linewidth);
```

```
ylim([0,450]);
xlim([0,60]);
xlabel('Time (ms)','FontSize',font);
ylabel('Torque (Nm)','FontSize',font);
legend('Conventional Motor','Proposed Motor');
set(gca,'FontSize',font,'LineWidth',linewidth);

set(gcf,'units','normalized','outerposition',[0 0 0.5 0.65])
saveas(gcf,  'Conventional Motor vs Proposed Motor Torque.jpg');
%close;
```

```
close all; clear; clc;
font=16;
linewidth=2;
T= xlsread('Current 19.23.xlsx');
x=T(:,1);
cur_a= T(:,2);
cur_b= T(:,3);
cur_c=T(:,4);

figure();
% subplot(3,1,1);
plot(x,cur_a,'r','LineWidth',linewidth);
 hold on;
plot(x,cur_b,'b','LineWidth',linewidth);
plot(x,cur_c,'k','LineWidth',linewidth);
ylim([0,25]);
xlim([0,60]);
xlabel('Time (ms)','FontSize',font);
ylabel('Current (A)','FontSize',font);

```

```
21 legend('Phase A','Phase B','Phase C');
22 set(gca,'FontSize',font,'LineWidth',linewidth);
23
24
25 set(gcf,'units','normalized','outerposition',[0 0 0.5 0.65])
26 saveas(gcf,  '19.23 Current.jpg');
27 close;
```

```
1 close all; clear; clc;
2 font=16;
3 linewidth=2;
4 T= xlsread('full.csv');
5 % x=T(:,1);
6   x=0:0.05:498.86;
7 tor= T(:,2);
8 tor=repmat(tor,2,1);
9 % f_tor= T(:,3);
10 % tor_1=f_tor/4;
11 % tor_2=f_tor/2;
12 figure();
13 % subplot(3,1,1);
14 plot(x,tor,'r','LineWidth',linewidth);
15 %  hold on;
16 %  plot(x,f_tor,'b','LineWidth',linewidth);
17 ylim([-50,500]);
18 xlim([0,500]);
19 xlabel('Rotation (degrees)','FontSize',font);
20 ylabel('Torque (Nm)','FontSize',font);
21 legend('Torque Profile');
22 set(gca,'FontSize',font,'LineWidth',linewidth);
23 set(gcf,'units','normalized','outerposition',[0 0 0.5 0.65])
```

```
24 saveas(gcf, 'Motor Torque for .5 sec .jpg');
25 %close;
```

Vita

Rochak Shiwakoti is an Electrical Engineering Masters student at the University of New Orleans, LA, USA. He received his Bachelor of Science in Electrical Engineering from University of New Orleans. He is currently working as a graduate research assistant with Dr. Parviz Rastgoufard, Dr. Ittiphong Leevongwat and Dr. Ebrahim Amiri in UNO Power and Energy Research Lab (PERL) located in Center for Energy Resource Management (CERM) building in Research and Technology Park at the University of New Orleans. His areas of research and interest include motor modeling, simulation, and power system engineering.